DEM MODELLING OF THE SHEAR BEHAVIOUR OF ROCK JOINTS

C. Lambert
Department of Civil & Natural Resources Engineering, University of Canterbury, Christchurch, New Zealand

C. Coll
Golder Associates Ltd, Christchurch, New Zealand

ABSTRACT: *The constitutive behaviour of rock discontinuities is highly controlled by the roughness of the surface. Its contribution is a combination of two aspects of overall roughness: the morphology of the surface (or shape) and the strength of the asperities (related to the strength of the surrounding rock). Appropriate description of rock joint behaviour entails accurate description of the morphology and provision for asperity degradation. In this study, we propose to take advantage of the latest developments in numerical techniques. The DEM code PFC3D has been used to generate a numerical replica of a joint. Microproperties have been calibrated to mimic the physical rock. The morphology has been obtained using 3D photogrammetry. The derived triangulated surface is then introduced into PFC3D to generate a synthetic rock joint. The recently developed Smooth Joint contact model is used to describe the interaction between particles lying on opposite side of the surface. The smooth joint model allows to get rid of the artificial roughness introduced by particle discretization. The generated discrete model replicates the two aspects of overall roughness: shape and strength. Direct shear tests are then performed to characterise its mechanical behaviour. Results of the simulations are presented.*

1 INTRODUCTION

The shear behaviour of discontinuities is primarily controlled by the surface roughness (Barton, 1973) which is commonly defined through an empirical parameter, the Joint Roughness Parameter or JRC. Initially estimated by visual comparison with standard roughness profiles, correlations between JRC and various statistical parameters or fractal dimension have been established (Tse & Cruden, 1979; Carr & Warriner, 1989). JRC based estimates offer simplicity of used however they are two dimensional methods and non directional. More recently the use of laser scanner and photogrammetry to define the surface topography and estimate the roughness have been described (Hans & Boulon, 2003; Haneberg, 2007). New constitutive relations have been developed based on a general description of roughness (Grasselli & Egger, 2003). Asperity shape and distribution on a discontinuity can now be measured with a great detail and potentially incorporated in any analysis. However with the complexity of the interaction between the two walls, a complete analytical formulation remains a hard task. Various constitutive models have been developed that accommodate effect of asperities (Saeb & Amadei, 1992) and their progressive degradation during shearing (Plesha, 1987; Hutson & Dowding, 1990). Despite being each time more advanced, these models still rely on empirical relations or simplified descriptions of the surface asperities. The recent development of a new contact model named “Smooth

Joint Model" (SJM) (Pierce *et al.*, 2007) in PFC3D where particles are allowed to slide past one another without overriding one another has been a major breakthrough to represent discontinuities as planar surfaces. With this new formulation, real surface morphologies can be introduced into DEM codes to generate numerical rock joint. Studies by Lambert *et al.* (2010) on the behaviour of a rock-concrete interface suggested that realistic shear behaviour, shear strength and dilation, could be obtained associating the SJM with a true morphology. Such synthetic rock joint is able to replicate the behaviour of its physical counterpart and can be used to estimate its constitutive behaviour accounting for the three dimensionality of the surface (Lambert & Coll, 2011). The behaviour of rough fractures can be explicitly simulated on the basis of measurable properties: 3D surface morphology and mechanical properties of the surrounding rock.

2 DISCRETE ELEMENT REPRESENTATION OF A ROCK JOINT

2.1 Smooth joint contact

A discontinuity is normally represented in PFC3D by debonding contacts along a surface. Previous modelling approaches used bands of particles with altered properties (Kulatilake *et al.*, 2001; Park & Song, 2010) to represent a joint. However, the particle geometry is still present and the discrete nature of the medium generates an artificial roughness that is added to the one of the introduced surface, thus creating a particle size dependent joint behaviour (see Fig. 1).

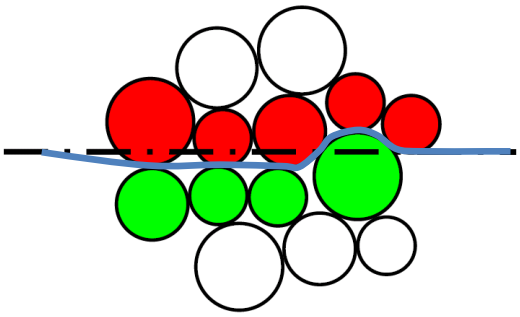

Fig. 1. 2D example of a particle size dependant surface morphology of joints (modified after Scholtes *et al.*, 2010)

In order to overcome the problem an alternate scheme, termed the "Smooth-Joint Model" or SJM, initially proposed by Pierce *et al.* (2007), has been implemented into PFC3D (Itasca, 2008). A smooth-joint model is a contact model that simulates the behaviour of an interface regardless of the local particle contact orientation along the interface. A typical smooth-joint is shown in Fig. 2. It allows particles to slide past one another without overriding one another. A joint is created by assigning this new contact model to all the contacts between particles that lie upon opposite sides of the surface. The SJM defines the tangential and normal directions according to the local orientation of the surface (by opposition to the initial normal and tangential directions of the contact, see Fig. 2). The joint normal and joint tangential force increments (ΔF_{nj} and ΔF_{tj} respectively) are derived from normal and tangential displacement increments (ΔU_{nj} and ΔU_{tj}) multiplying by the joint stiffness ($\Delta F_{nj} = k_{jn}\Delta U_{nj}$ and $\Delta F_{tj} = k_{jt}\Delta U_{tj}$). The joint force is then adjusted to satisfy the force-displacement relationship and mapped back into the global system. This new formulation accommodates the standard behaviour of a joint (sliding/opening behaviour) independently of particle

induced roughness. A complete description of the formulation can be found in the manual (Itasca, 2008).

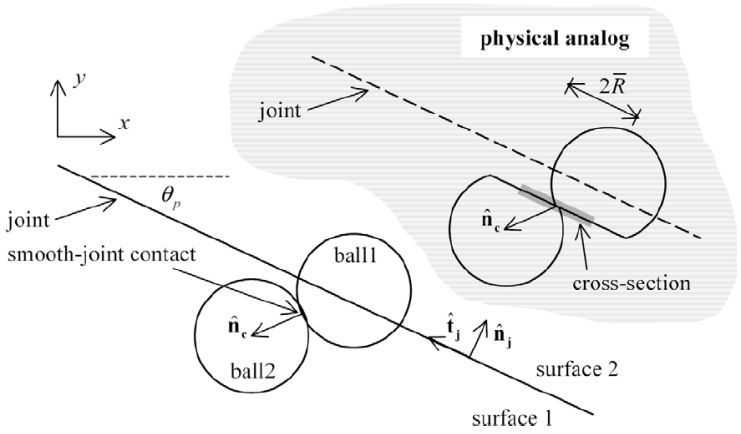

Fig. 2. Smooth Joint contact model between ball 1 and ball 2. Surface 1 and surface 2 denote either side of the joint lying at a dip angle of θ_p (after Itasca, 2008)

The model requires the definition of a set of parameters: friction coefficient, dilation angle, normal and shear bonds (responsible for cohesion), normal and shear stiffness. This new formulation has proven its ability to capture the behaviour of jointed rock mass representing joints as planar surfaces (Pierce *et al.*, 2007; Deisman *et al.* 2010; Esmaieli *et al.*, 2010; Lambert & Read, 2011) and the behaviour of rough discontinuities (Lambert *et al.*, 2010, Lambert & Coll, 2011).

2.2 3D morphology of the rock joint

The interface morphology used in this example is based on a natural discontinuity in granite studied by Grasselli (2001). The surface is 140× 140 mm^2 and the maximum amplitude of the asperities is around 9 mm. Fig. 3 shows a general view of the surface. The three dimensional surface has been triangulated using a Kriging gridding method with a horizontal spacing of 1.4 mm between the grid points (in x and y directions). 99 profiles along the x axis and y axis have been extracted for which Z_2 coefficients (root mean square of the first derivative of the profile) have been estimated:

$$Z_2 = \sqrt{\frac{1}{(N-1)\Delta x^2}\sum_{i=1}^{N-1}(z_{i+1}-z_i)^2} \tag{1}$$

where z_i and z_{i+i} are the elevations of two consecutive grid points on a profile, N the total number of grid points on a profile and Δx the horizontal spacing.

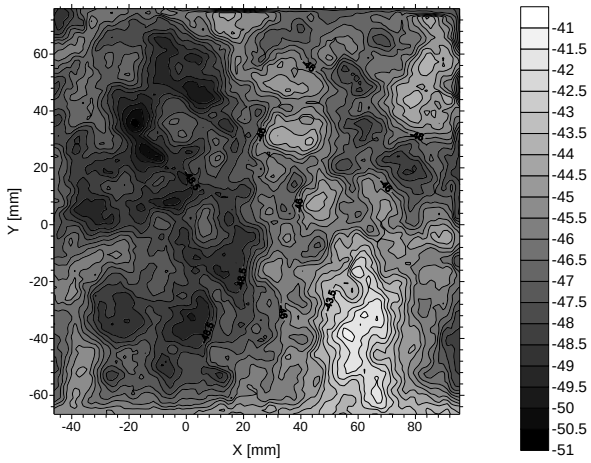

Fig. 3. Morphology of the granite surface (modified from Grasselli (2001))

For each profile a value of the Joint Roughness Coefficient (JRC) can be derived using the empirical relation proposed by Yang *et al.* (2001).

$$JRC = 32.69 + 32.98 \times \log_{10}(Z_2) \tag{2}$$

The profiles of the triangulated surface exhibited in along x axis an average JRC_{prof} of 10.4, varying from 4.9 to 13.9 and along y axis an average of 10.1, varying from 5.7 to 15.3. The cumulative distribution of the JRC_{prof} is given in Fig. 4

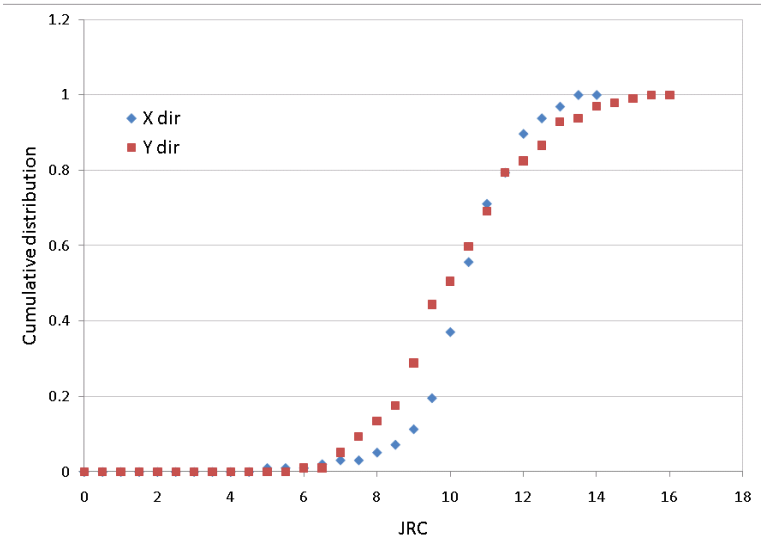

Fig. 4. Cumulative distribution of JRC values along x direction and y direction.

2.3 The synthetic rock joint

A synthetic (or numerical) rock joint is obtained first generating a particle assembly using a discrete element code and then introducing the surface morphology. Micro-properties of the particle assembly are calibrated to match the properties of the physical material (surrounding rock) following the genesis procedure described in detail in Potyondy & Cundall (2004). In

that case a granitic rock with a UCS of 143MPa has been simulated. The numerical rock joint consists of a 140 x 140 x 50mm3 (respectively X, Y, Z) parallelepiped particle assembly. The final specimen contains 98,345 particles having a radius ranging from 0.5mm (in the vicinity of the interface) to 2.4mm. The triangulated surface of the joint presented in the previous section is then imported. For each triangle a "smooth joint model" is assigned to the contacts between particles that lie on opposite side of a triangle. The orientation of the smooth joint corresponds to the orientation of the triangle. The joint surface is hence modelled as a collection of smooth-joint contacts with varying orientation. The macroscopic joint is considered to be purely frictional at the contact level (smooth joint) with a friction angle of 20°. No dilation was introduced as macroscopic dilation (i.e. at the joint level) is expected to be an emergent property of the surface topology.

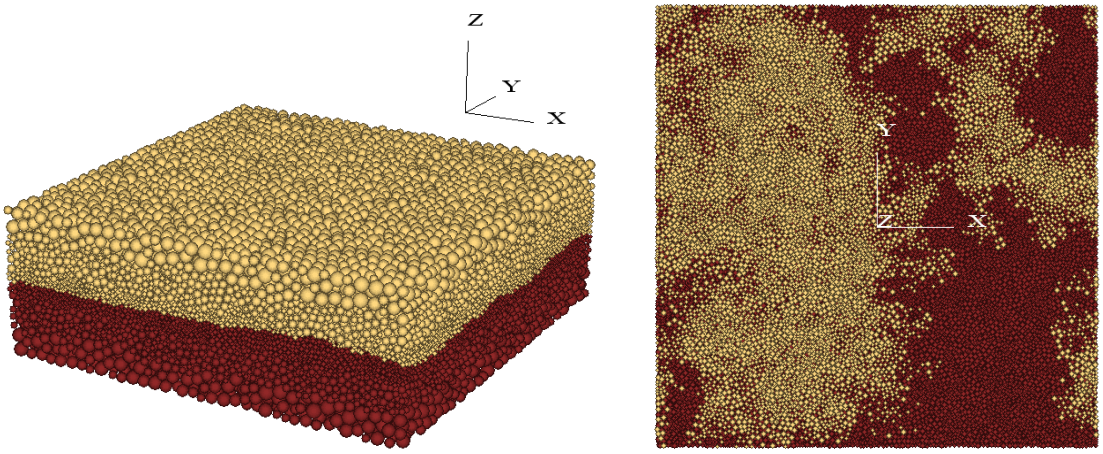

Fig. 5. Visualization of the synthetic rock joint sample. Upper wall in orange and lower wall in brown. Full 3D view on the left and lower half section on the right

3 SHEAR BEHAVIOUR OF THE SYNTHETIC ROCK JOINT

3.1 Simulations of direct shear tests

Numerical shears tests under constant normal stress have been performed on the synthetic rock joint for three values of normal confinement (0.5MPa, 1MPa, 1.5MPa). The specimen is firstly subjected to a compression along axis Z (Fig. 5) and then to a shearing along axis X at constant normal stress. Displacements along Y are restrained. The sum of contact forces on the periphery of the upper half are used to compute the average normal stress and shear stress on the interface whereas normal and tangential displacements are monitored averaging particle displacements on the periphery of the lower half (Z displacements and X displacements respectively).

Fig. 6(a) and (b) show the evolution of shear stress and normal displacement with shear displacement. It can be seen that the classical elasto-plastic response of rock joints is well captured. The mobilised shear stress increases to a peak value as roughness is mobilised and then decreases due to asperity degradation. The peak value defines the shear strength of the synthetic rock joint (the higher the normal stress, the higher the shear strength). Peak dilation angles have been measured as the slope of the normal displacement vs. shear displacement curve at the peak of the shear stress (Fig. 6). As shown in Fig. 6, dilation decreases as normal stress increases.

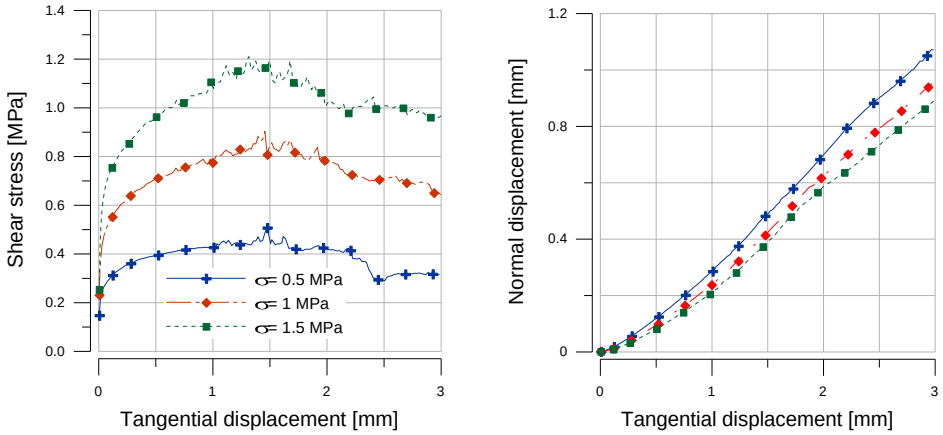

Fig. 6. Stress-displacement curves of direct shear tests under constant normal stress (ranging from 0.5 MPa to 1.5 MPa) on a 140 x 140 mm2 surface. a) Shear stress versus tangential displacement. b) Normal displacement versus tangential displacement.

The numerical shear tests performed under increasing normal stress define the strength envelope of the model from which a Barton failure criterion (Barton & Choubey, 1977) can be expressed. In Barton's formulation the shear strength is expressed as a function of the Joint Roughness Coefficient (JRC), Joint Compressive strength (JCS) and friction ϕ_b (3):

$$\tau_p = \sigma_n \cdot \tan\left(JRC \cdot \log_{10}\left(\frac{JCS}{\sigma_n} \right) + \phi_b \right) \tag{3}$$

Where τ_p is the peak shear stress and σ_n the normal stress.

A best fit of Barton's failure criterion can be seen on Fig. 7. The base friction angle ϕ_b in equation (1) corresponds to the friction angle of a perfectly planar discontinuity and corresponds to the friction angle of the in the smooth joint model (20°). *JCS* has been set to 143 MPa. The best fit returns a JRC_{back} of 9.9 with a coefficient of determination R^2 close to 1. Obtained JRC_{back} is in good agreement with the average JRC_{prof} determined on 2D profiles of the surface suggesting that the effect of roughness is well captured.

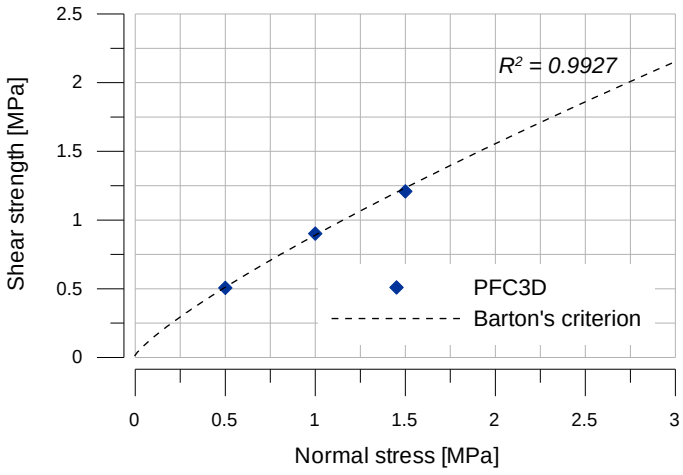

Fig. 7. Failure criterion for the synthetic rock joint with a best fitted Barton criterion (*JRC = 9.9)*

3.2 Shear strength anisotropy

Anisotropy in the shear behaviour induced by surface roughness is assessed by shearing the synthetic rock joint varying the direction of loading. Two series of direct shear tests have been performed along the x axis, towards x>0 and x<0. A series of shear tests have been performed along the y direction towards y>0. The three directions tested will be referred to as 0°, 90° and 180° for x>0, y>0 and x<0 respectively. The shear strength for the various tests are plotted in Fig. 8.

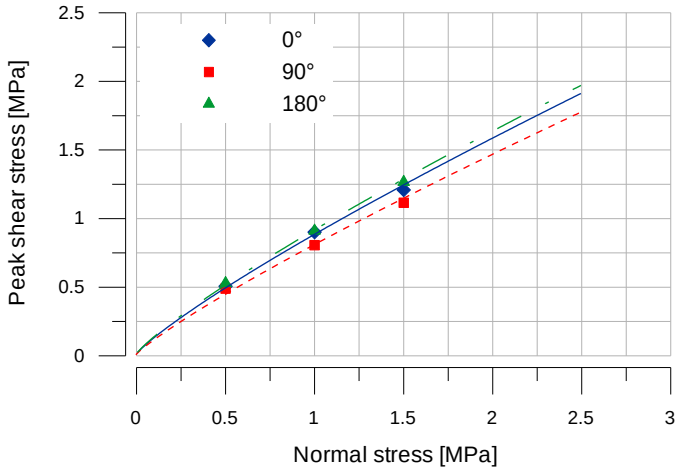

Fig. 8. Anisotropy in the peak shear strength of the synthetic rock joint

The joint strength exhibits little various between the three shearing directions. The strength is slightly lower for 90° which is consistent with a slightly lower average JRC. The relatively small difference in the strength is also apparent in the average JRC.

4 CONCLUSION

A DEM approach was developed to generate a synthetic rock joint combining a real surface morphology with a smooth joint contact model at the particle level. Unlike previous discrete approaches, such numerical model is able to mimic the mechanical behaviour of a discontinuity qualitatively and quantitatively. Direct shear tests under constant normal stress have been performed and the mechanical response of the model has been analysed. The effect of roughness was consistently captured throughout the simulations. Strength estimates can be performed with this approach accounting for the 3D aspect of surface roughness and properties such as anisotropy can be captured.

ACKNOWLEDGMENT

The authors would like to thank Dr. Giovanni Grasselli for providing the natural morphology of a discontinuity in granite.

REFERENCES

Barton, N. (1973), “Review of a new shear-strength criterion for rock joints”, Eng. Geol., Vol. 7(4), 287–332.

Barton, N. & Choubey, V.(1977), “The shear strength of rock joints in theory and practice”, Rock Mechanics, Vol. 10, 1-54.

Carr, J.R. & Warriner, J.B. (1989), "Relationship between the fractal dimension and joint roughness coefficient", Bull. Association of Engineering Geologists, XXVI(2), 253-263.

Deisman, N., Mas Ivars, D., Darcel, C., & Chalaturnyk, J. (2010), "Empirical and numerical approaches for geomechanical characterization of coal seam reservoirs", International Journal of Coal Geology, Vol. 82, 2204-212.

Esmaieli, K., Hadjigeorgiou, J. & Grenon, M. (2010), "Estimating geometrical and mechanical REV based on synthetic rock mass models at Brunswick Mine", Int. J. Rock Mech. Min. Sci., Vol. 47, 915–920.

Grasselli, G. (2001), "Shear strength of rock joints based on quantified surface description", Ph.D. thesis, Ecole Polytechnique Fédérale de Lausanne, Switzerland.

Grasselli, G. & Egger, P. (2003), "Constitutive law for the shear strength of rock joints based on three-dimensional surface parameters", Int. J. Rock Mech. Min. Sci., Vol. 40, 25–40.

Haneberg, W.C. (2007), "Directional roughness profiles from three-dimensional photogrammetric or laser scanner point clouds", In Rock Mechanics: Meeting Society's Challenges and Demands, 1st Canada–US Rock Mechanics Symposium, Vancouver, 101-106.

Hans, J. & Boulon, M. (2003), "A new device for investigating the hydromecanical properties of rock joints", Int. J. Rock Mech. Min. Sci., Vol. 27, 513-548.

Hutson, R. & Dowding, C. (1990), "Joint asperity degradation during cyclic shear", Int. J. Rock Mech. Min. Sci. Geomech. Abstr., Vol. 27, 109–119.

Itasca Consulting Group (2008), "Particle Flow Code in 3 Dimensions, version 4.0".

Kulatilake, P., Malama, B. & Wang, J. (2001), "Physical and particle flow modeling of jointed rock block behavior under uniaxial loading", Int. J. Rock Mech. Min. Sci., Vol. 38, 641–657, 2001.

Lambert, C., Buzzi, O. & Giacomini, A. (2010), "Influence of calcium leaching on the mechanical behavior of a rock mortar interface: a dem analysis", Computers and Geotechnics, Vol. 37, 258-266.

Lambert, C. & Coll, C. (2011), "A synthetic rock joint for joint strength estimates", Int. J. Rock Mech. Min. Sci., submitted.

Lambert, C. & Read, J. (2011), "Sensitivities in Sensitivities in rock mass properties: A DEM insight", European Journal of Environmental and Civil Engineering, 2011.

Park, J.-W. & Song, J.-J. (2010), "Numerical simulation of a direct shear test on a rock joint using a bonded-particle model", Int. J. Rock Mech. Min. Sci., Vol. 46, 1315-1328, 2010.

Pierce, M., Cundall, P., Potyondy, D. & Mas Ivars, D. (2007), "A Synthetic Rock Mass Model for Jointed Rock", In Rock Mechanics: Meeting Society's Challenges and Demands, 1st Canada–US Rock Mechanics Symposium, Vancouver, 341–349.

Plesha, M. (1987), "Constitutive models for rock discontinuities with dilatancy and surface degradation", International journal for numerical and analytical methods in geomechanics, Vol. 11, 345–362.

Potyondy, D.O. & Cundall, P.A. (2004), "A bonded-particle model for rock", Int. J. Rock Mech. Min. Sci., Vol. 41, 1329-1364.

Saeb, S. & Amadei, B. (1992), "Modelling rock joints under shear and normal loading", Int. J. Rock Mech. Min. Sci., Vol. 29, 267–278.

Scholtes, L., Donze, F.V. & Read, J. (2010), "3D DEM modelling of jointed rock slopes", in Rock Slope Stability Symposium RSS 2010, 2010.

Tse, R. & Cruden, C.M. (1979), "Estimating joint roughness coefficients", Int. J. Rock Mech. Min. Sci., Vol. 32, 303-307.

Yang, Z.Y., Di, C.C. & Yen, K.C. (2001), "The effect of asperity order on the roughness of rock joints", Int. J. Rock Mech. Min. Sci.,, Vol. 38, 745-752.